Research Square

Preprints are preliminary reports that have not undergone peer review.
They should not be considered conclusive, used to inform clinical practice,
or referenced by the media as validated information.

The Triad of Frailty, Tumor Neglect, and Operative Burden in Extensive Scalp Reconstruction: A 10-Year Experience with Rare Diagnoses

Ömer Faruk Dilek

omerfaruk.dilek@sbu.edu.tr

University of Health Sciences, Şişli Hamidiye Etfal Training and Research Hospital, Istanbul, Turkey

Murat Doğuş Çerikan

University of Health Sciences, Şişli Hamidiye Etfal Training and Research Hospital, Istanbul, Turkey

Soysal Baş

Balıkesir Atatürk City Hospital

Buket Bambul

University of Health Sciences, Şişli Hamidiye Etfal Training and Research Hospital

Selman Hakkı Altuntaş

Süleyman Demirel University

Yiğit Arslan

Süleyman Demirel University

Kamuran Zeynep Sevim

University of Health Sciences, Şişli Hamidiye Etfal Training and Research Hospital, Istanbul, Turkey

Research Article

Keywords: Proliferating trichilemmal tumor, Dermatofibrosarcoma protuberans, Pilomatrixal carcinoma, Hidradenocarcinoma, Syringocystadenocarcinoma papilliferum, Skin cancer, Scalp reconstruction, Tumor neglect, Frailty, Modified frailty index

Posted Date: October 29th, 2026

DOI: https://doi.org/10.21203/rs.3.rs-10942575/v1

License: This work is licensed under a Creative Commons Attribution 4.0 International License.
Read Full License

Additional Declarations:
No competing interests reported.

Table 1 to 4 are available in the Supplementary Files section.

The Triad of Frailty, Tumor Neglect, and Operative Burden in Extensive Scalp Reconstruction: A 10-Year Experience with Rare Diagnoses

Key Words

Proliferating trichilemmal tumor; Dermatofibrosarcoma protuberans; Pilomatrixal carcinoma; Hidradenocarcinoma; Syringocystadenocarcinoma papilliferum; Skin cancer; Scalp reconstruction; Tumor neglect; Frailty; Modified frailty index

Title Page

Title: The Triad of Frailty, Tumor Neglect, and Operative Burden in Extensive Scalp Reconstruction: A 10-Year Experience with Rare Diagnoses

Authors:

Ömer Faruk Dilek[1]*

ORCID: 0000-0001-9650-3806; Email: omerfaruk.dilek@sbu.edu.tr

Murat Doğuş Çerikan[1]

ORCID: 0000-0001-6121-2734 ; Email: muratdogus98@gmail.com

Soysal Baş[2]

ORCID:0000-0002-4657-1613; Email: soysalbas@gmail.com

Buket Bambul[3]

ORCID: 0000-0001-5400-5534; Email: buketbambul@hotmail.com

Selman Hakkı Altuntaş[4]

ORCID: 0000-0002-9577-7052; Email: shaltuntas@gmail.com

Yiğit Arslan[4]

ORCID: 0000-0002-2837-048X; Email: yigitarslan.md@gmail.com

Kamuran Zeynep Sevim[1]

ORCID: 0000-0002-9625-6670 ; Email: kzeynep.sevim@gmail.com

Affiliations:

[1] Department of Plastic, Reconstructive and Aesthetic Surgery, University of Health Sciences, Şişli Hamidiye Etfal Training and Research Hospital, Istanbul, Turkey

[2] Department of Pathology, University of Health Sciences, Şişli Hamidiye Etfal Training and Research Hospital, Istanbul, Turkey

[3] Department of Plastic, Reconstructive and Aesthetic Surgery, Balikesir City Hospital, Balikesir, Türkiye

[4] Department of Plastic, Reconstructive and Aesthetic Surgery, Süleyman Demirel University, Isparta, Turkey

***Corresponding author:** Ömer Faruk Dilek, Department of Plastic, Reconstructive and Aesthetic Surgery, University of Health Sciences, Şişli Hamidiye Etfal Training and Research Hospital, Istanbul, Turkey. Email: omerfaruk.dilek@sbu.edu.tr

ABSTRACT

BACKGROUND

Elderly, debilitated patients are increasingly challenged by advanced, untreated scalp cancers presenting with significant tumor burdens, physical frailty, and demanding reconstructive needs. Surgeons face the difficult balance of providing curatively radical surgery while managing the physiological constraints of these vulnerable individuals.

METHODS

We performed a retrospective review of 34 patients with extensive neglected scalp malignancies (defect >50 cm^2) treated surgically between 2015–2025. Preoperative frailty was evaluated using the modified Frailty Index-5 (mFI-5). Overall Surgical Oncologic Clearance (OSOC) was determined via multidisciplinary consensus incorporating intraoperative visualization, frozen sections, and final pathology. Reconstructive plans were individualized, prioritizing extended local or regional flaps and avoiding free tissue transfer when oncological and technically feasible. Survival was analyzed using Kaplan-Meier estimates and log-rank tests. A ridge-penalized Cox Proportional Hazards Model, validated by two independent statistical methodologies, was utilized to identify independent predictors of disease-specific mortality.

RESULTS

Twenty-seven (79%) patients had NMSCs (21 SCC, 6 BCC). Most of these patients were highly frail (mean mFI-5 = 2.8 ± 0.8). Disease-specific mortality was significantly higher following unsuccessful OSOC compared to successful OSOC (80% vs. 4.5%, p = 0.001). Achieving successful OSOC remained independently associated with improved survival, even after accounting for frailty and operative burden (HR = 0.25; 95% CI 0.06–1.00; p = 0.05). Utilizing extended local and regional flaps successfully closed massive defects up to 251.2 cm2 without

increasing the rates of failed OSOC compared to free flap reconstruction (81.8% vs. 80%, p = 1.0). The remaining seven patients presented with rare, difficult-to-diagnose pathologies including proliferating trichilemmal tumor, dermatofibrosarcoma protuberans, pilomatrixal carcinoma, malignant melanoma, hidradenocarcinoma, and syringocystadenocarcinoma papilliferum.

CONCLUSIONS

Complete oncologic clearance, rather than frailty status alone, remains the most important factor determining disease-specific survival in patients with neglected scalp malignancies. Furthermore, extending the reconstructive ladder to favor larger local and regional flaps reduces operative burden without decreasing the success rates of oncologic clearance. Therefore, a curative-intent approach is advocated for frail geriatric patients, provided the reconstructive strategy minimizes operative risk. Finally, large, atypical masses with indeterminate initial biopsies warrant particular caution, as non-diagnostic results may obscure aggressive rare pathologies.

I. Introduction

The management of advanced scalp malignancies is often complicated by "tumor neglect" — a delay in seeking medical care due to psychosocial barriers, cognitive impairment, denial, and socioeconomic limitations[1-3]. When untreated, these lesions can reach "giant" size: over 5 cm for non-melanoma skin cancers (NMSC)[4, 5]—specifically basal cell carcinoma (BCC) and squamous cell carcinoma (SCC)—or 10 cm for malignant melanomas (MM)[6]. This extreme neglect occurs especially in elderly patients with physical and cognitive frailty[2, 7] who already bear reduced functional reserve and multiple comorbidities. Extirpating these neglected lesions requires a demanding surgical spectrum, varying from challenging defects, such as completely removed periosteum in the mildest scenarios or more complex examples mandating calvarial and dural resection and reconstruction. Specifically, for scalp defects exceeding 50 cm^2 with prominent bone exposure, classical algorithms[8, 9] strongly advocate microvascular free tissue transfer as the gold standard to achieve stable, well-vascularized closure. The clinical feasibility of applying such a wide range of surgical interventions to a frail and vulnerable population has become a key topic of discussion[10]. The practice of subjecting this specific patient demographic to complex, long-hour microsurgical procedures has given rise to significant clinical and ethical concerns within the field of geriatric oncology[10, 11]. These debates also complicate therapeutic decisions for clinicians. They have to weigh the increased surgery-related mortality risk caused by frailty against the biologic behaviour of many of these relatively slow-growing, indolent tumors. More specifically, there is increasing concern that the high operative burden resulting from aggressive, prolonged interventions may ultimately compromise a frail patient's residual physical reserves; meaning that patients might actually live longer if the underlying cancer were left to its natural history.

Over the past decade, our practice regarding the high operative burden in frail patients has evolved around two clear principles: (1) Oncological clearance must be maintained as strictly as possible. At the same time, a patient's frailty cannot be ignored. Balancing these two needs calls for an individualized reconstructive approach. (2) Reconstruction is the most flexible part of the surgical plan, so this is where individualization matters most. However, this flexibility is not also without risks. A poorly chosen or partially failed reconstruction, such as graft loss or flap necrosis, adds a serious extra burden to an already vulnerable patient. In this study, we report the reconstructive, oncological, and histopathological outcomes of neglected scalp tumors. We also describe key operative parameters and share our experience with the rare malignancies that met our strict inclusion criteria. This experience especially highlights the diagnostic and histopathological complexity of this patient group.

II. Material and Method

1. Study Design and Patient Selection

This is a retrospective cohort study. During the study period, standard-of-care oncological clearance and immediate reconstruction were uniformly offered to all patients presenting with neglected scalp tumors, irrespective of chronological age or apparent physical frailty. Patients who consented to the proposed surgical intervention were included in the study. To critically evaluate the outcomes of these uniform surgical decisions within the context of current geriatric oncology debates, patient frailty was assessed strictly on a retrospective basis using the modified Frailty Index-5 (mFI-5)[12, 13]. Data regarding the five constituent variables (diabetes mellitus, hypertension, history of COPD (chronic obstructive pulmonary diseases) /severe pneumonia, history of congestive heart failure, and non-independent functional status) were extracted from historical preoperative records. Rather than relying on a diameter-based threshold, inclusion was defined by a defect area exceeding 50 cm^2, a cutoff selected specifically to capture cases posing a strict reconstructive challenge, irrespective of the precise tumor diameter.

2. Data Extraction and Psycho-Social Stratification

Data collection included a detailed examination of all patient charts and electronically available medical records, surgical reports, and histopathologic analyses. When the exact timeline of diagnostic delay or the specific psychosocial drivers of neglect were not clearly documented, we conducted supplementary telephone interviews with patients or their primary caregivers. With their consent, this information was also cross-checked by accessing the centralized national health system database. This allowed us to confirm diagnostic and treatment dates, cause of death, and long-term vital status with a higher level of accuracy than patient or caregiver declarations alone could provide. Patients whose current vital status could not be clarified through these methods, or whose relatives refused to share information (n=5; 4 SCC and 1 angiosarcoma of the scalp), as well as one patient who accepted the initial intervention offer only after six months (n=1, SCC), were excluded from the study.

We classified the underlying reason for neglect using a psycho-social framework developed for delayed presentation in advanced skin cancer[2]. This framework groups neglect into six categories: (1) negligence or denial, often linked to cognitive impairment, psychiatric illness, or substance use; (2) avoidance, including hiding the lesion or withdrawing from social and medical contact; (3) misinterpretation of symptoms (banalization, BN), where a slow-growing or painless lesion was mistaken for something benign; (4) fear (FR) or shame, centered on the diagnosis itself or the prospect of disfiguring treatment; (5) access barriers to healthcare, such as socioeconomic or geographic constraints; and (6) caregiver-dependent (CD) neglect, where responsibility for seeking care had effectively passed to a caregiver who did not act in time. Extracted data included patient demographics, preoperative tumor dimensions, major complications, this psychosocial classification of tumor neglect, and definitive verification of long-term vital status, exact cause of death, and other critical prognostic variables.

3. Staging, Surgical Approach and Reconstructive Strategy

We conducted wide local excisions for all clinically staged T3 non-melanoma skin cancers. These excisions included removal of the periosteal layer beneath the tumor, regardless of whether this resulted in a more complex defect; intraoperative frozen sections were utilized as needed to assess margins. Our ten-year study spanned a period of changes in how both clinical staging and risk classification were assessed. These changes included the transition from the AJCC 7th to the AJCC 8th edition (updated in 2017-18), and the NCCN's adoption of a 3-tiered risk assessment model for non-melanoma skin cancer (in 2022). For consistency, we restaged all tumors using the AJCC 8th edition criteria, while neck management decisions followed the standard of care at the time of each patient's treatment. More specifically, patients with T4 tumors, or T3 tumors with clinical nodal disease, underwent simultaneous therapeutic regional dissection (RD; neck dissection ± parotidectomy). In clinically node-negative (cN0) T3 cases, our protocol favored elective RD when final histopathology showed at least two high-risk features. This threshold was our institutional practice throughout the study period, applied well before the NCCN introduced a comparable 'multiple risk factors' pathway in 2022, with which our protocol was found to be concordant.

For lesions with an unclear initial diagnosis (Nd or mNd), or rare tumor types with no established margin guidance, we used a default 2-cm margin. These lesions were managed with the same caution as confirmed high-risk malignancies until definitive histopathology was available.

When multiple reconstructive options were available, decision-making was tailored pragmatically based on the cumulative clinical experience of the surgical team. Selection was guided by patient-specific and logistical factors, including the ASA physical status, existing comorbidities, anticipated intensive care unit (ICU) requirements, estimated operative duration, and the availability of the microsurgical team. Regardless of the chosen modality, the goal was to achieve a definitive, single-stage reconstruction that minimized postoperative wound care and eliminated the need for revisions. Operative variables (surgical duration, reconstructive modality, concurrent calvarial resection, complications, and length of hospital stay) were systematically recorded. The surgical defect area was calculated using the formula for an ellipse: $\pi \times a/2 \times b/2$ (where a and b represent the maximum longitudinal and transverse orthogonal diameters).

4. Pathological Evaluation and Follow-up

Definitive pathological evaluation systematically documented the primary and definitive histological diagnosis, histological subtype, tumor grade, definitive pathological staging, and the maximum depth of microscopic invasion. Furthermore, high-risk features (e.g., perineural and lymphovascular invasion) alongside precise assessments of both deep and lateral surgical margins were recorded.

The periosteum is not simply a passive tissue plane. It has been shown to act as an active stromal barrier, that can limit, and can locally arrest, tumor invasion into the underlying bone[14, 15]. Tumor continuity with the periosteum, therefore, does not automatically mean the cortex has been invaded. Furthermore, cortical bone provides a further layer of resistance. Its dense, lamellar architecture impedes and slows direct tumor spread, in contrast to soft tissue, where tumors spread much more freely[16-18]. As a result, true bony invasion tends to proceed gradually through a resorption-dependent process rather than free extension. This structural distinction has a practical consequence. The extent of periosteal and

cortical involvement, and the appropriate depth of bone intervention, can often be judged reliably through direct intraoperative macroscopic assessment[19-21]. For these reasons, across our 10-year experience, decisions regarding subsequent treatment modalities were guided not by the conventional R0/R1/R2 margin classification but by an integrated "overall surgical oncologic clearance" (OSOC) assessment, determined for each case by the multidisciplinary tumor board, including the patient's own surgeon, at the time definitive pathology became available. This assessment incorporated the intraoperative macroscopic evaluation of distinct anatomical layers, the findings of any intraoperative frozen section analysis, and the final permanent pathology report. We therefore report oncologic outcomes in the present study using this same OSOC framework, consistent with how treatment decisions were actually made in clinical practice. Following two scenarios illustrate our OSOC application in practice. First, in excisions involving the periosteum where the calvarial bone appeared macroscopically normal, OSOC was considered achieved even if permanent pathology later showed the tumor in continuity with the periosteum. Second, when cortical involvement was identified and adequately treated with burring, OSOC was likewise considered achieved, again regardless of any periosteal continuity noted on final pathology.

Strict oncological surveillance data were gathered to evaluate long-term outcomes. The primary prognostic endpoints included local recurrence (LR), regional lymph node metastasis, distant metastasis (dm), and Tumor-Free Survival (TFS). Total follow-up duration was calculated in months from the date of the primary ablative surgery to the most recent clinical encounter or documented death. Patient survival status at the final contact was explicitly categorized into one of three definitive outcomes: Alive, Dead of Disease (DOD), Dead of Other Causes (DOC).

5. Statistics

Statistical analyses were performed to evaluate the multifactorial determinants of operative burden and survival. Descriptive statistics for continuous variables were reported as mean ± standard deviation (SD). Continuous variables were compared across independent groups using the non-parametric Mann-Whitney U test, appropriate given the limited sample size (NMSC subgroup, n=27). Categorical variables were analyzed using Fisher's Exact test. Univariate survival analysis was conducted using the

Kaplan-Meier method, and differences in survival distributions (DOD, DOC, and TFS) were assessed via the Log-rank test.

A multivariate ridge (L2)-penalized Cox proportional hazards regression model was created to estimate independent predictors of disease-specific mortality in relation to the mFI-5 and operative time. As the number of events was low (n=5), the penalization parameter λ (a priori set at 1.0) could not be reliably estimated by cross validation; instead, it was conservatively used as a default value. In addition to addressing the problem of few observations due to the small sample size, penalization also helped resolve quasi-complete separation, which would have led to the estimation of non-sensible values for the HRs; the standard errors for these estimates would likely have been inflated. This is confirmed by comparing an unpenalized model (fit for comparison using R's survival package) that gave a very implausible OSOC hazard ratio (0.001, 95% CI [$1.6 \times 10{-}6$ – 0.7]) with a large standard error (3.31). The confidence interval for the penalized model is based on the penalized Hessian (thus Wald-type) and therefore only approximate.

Our main model was written as a custom python 3.10 code. In order to determine that the results from the primary model were not due to an issue in our programming, we re-fitted the same model twice using other well-established software package. Specifically, we used *Python's lifelines v0.30.0* and *R's survival* package (with a ridge penalty term) in *coxph*. Since there is no standardization for the relative size of a ridge penalty term between different statistical software packages, we did not expect the exact magnitude of the OSOC effect to be identical among all three models. Instead, we sought to confirm whether the direction and the overall level of the OSOC effect were consistent regardless of which model was used. We report these comparisons to our original model in **Table 4.** Statistical significance for the primary analysis was defined as a two-tailed $p < 0.05$.

Use of Artificial Intelligence-Assisted Technologies

During the preparation of this manuscript, the authors used an AI-based language model (Claude, Anthropic) to assist with Python syntax used in the statistical analysis, and for English-language review, including reducing word count and, in select instances, achieving more accurate emphasis of intended

meaning. All AI-assisted content was reviewed and verified by the authors, who take full responsibility for the accuracy, integrity, and originality of the final manuscript.

Results

Between 2015 and 2025, a total of 34 patients (18 males, 16 females; mean age 71.5 years) who underwent surgical resection and reconstruction were included, with clinical and histopathological data summarized in **Tables 1** and **2**. Delayed medical presentation was primarily caused by CD neglect (n=27). Preliminary incisional biopsies occasionally failed (Nd, mNd) to reflect the true aggressiveness of the final pathology, leading to significant diagnostic conflict; notably, an initial biopsy indicating a benign syringocystadenoma papilliferum (SCAP) was revised to a malignant syringocystadenocarcinoma papilliferum (SCACP) following definitive excision. Other ambiguous preliminary reports were ultimately finalized as rare, aggressive neoplasms, including pilomatrixal carcinoma (PMC), MM, and hidradenocarcinoma (HAC). Ultimately, the definitive histopathological diagnoses were predominantly SCC (n=21) and BCC (n=6), which were specifically grouped into an NMSC subgroup (n=27) to ensure methodological homogeneity and allow for accurate survival analyses. The remainder of the cohort consisted of other rare pathologies, including proliferating trichilemmal tumor (PTT) and dermatofibrosarcoma protuberans (DFSP).

The reconstructive approach corresponded to the defect size for all 34 patients (**Figure 1**). In this context, operative time includes only the actual resection and reconstruction, leaving out the extra hours caused by major complications. An overlap segment emerged for defects between 62.8 and 86.35 cm^2 (n=12), where local flaps (LF, n=6, 50.0%), regional flaps (RF, Trapezius flap, n=4, 33.3%), and free flaps (FF, n=2, 16.7%) were all used. Below this range (≤62.7 cm^2; n=13), local flaps predominated (n=12, 92.3%), with a single regional flap (n=1, 7.7%, Patient #28) and no free flaps. Above it (>86.35 cm^2; n=9), free flaps were used in 55.6% of cases (n=5), with local flaps viable for the rest (n=4, 44.4%) and no regional flaps in this range.

Using the full cohort (n=34), operative time, hospital stay, and major complications — defined as any complication requiring a return to the operating room under general anesthesia — varied by

reconstructive modality and RD status (Table 3). Adding an RD roughly tripled operative time across reconstructive modalities, extending mean operative time from 145.6 ± 73.7 minutes without RD (n=24) to 322.0 ± 99.9 minutes with RD (n=10). Complications directly prolonged hospital stays across groups, though none arose from the RD procedure itself; the free-flap groups carried the highest complication rates (Table 3). OSOC achievement did not differ significantly between local/regional (81.8%) and free-flap (80.0%) reconstruction in the NMSC subgroup (Fisher's exact p = 1.0). Choosing local or regional flaps over free tissue transfer therefore did not cost oncological safety.

This NMSC subgroup (n=27) carried a markedly vulnerable comorbidity and frailty profile, with a mean mFI-5 score of 2.8 ± 0.8. Survival tracked closely with frailty, OSOC status, and cumulative operative time, which includes the management of major complications (**Figure 2**). Patients who died early (≤6 months; Patients #4, #8, #13, #20) were frailer (mean mFI-5 3.5 vs. 2.7) and carried a higher operative burden (355.0 vs. 171.5 minutes) than the rest of the cohort. Across the full subgroup, OSOC failure (n=5) carried an 80.0% disease-specific mortality (DOD) rate, versus just 4.5% when OSOC was achieved (n=22; Fisher's exact p = 0.001).This gap was mirrored in survival duration: patients who died of disease declined faster (mean TFS 3.3 ± 5.2 months, n=5) than those who died of other causes (16.7 ± 13.0 months, n=9; p = 0.031), while patients with successful OSOC survived a mean of 25.7 ± 19.1 tumor-free months — together pointing to a durable survival benefit from oncological clearance in this frail population.

Grouping patients by frailty clarified these findings (**Figure 3**). All five OSOC failures occurred in severely frail patients (mFI-5 ≥ 3; Patients #8, #10, #12, #13, #20), who also carried a high mean operative burden (292.0 minutes). Among severely frail patients who did achieve OSOC (n=11), DOD fell to 9.1% at a lower mean burden (181.8 minutes); the rest of this group (54.5%) died of other causes. Moderately frail patients (mFI-5 = 2, n=11) uniformly achieved OSOC, with 0% DOD, 72.7% survival at a median of 31 months, and a lower mean burden still (173.2 minutes).

Finally, we developed a penalized Cox model in the NMSC subgroup (n = 27; five disease-specific deaths) to see if there is evidence that OSOC predicts survival even after adjusting for frailty and the overall burden of surgery. Patients with successful OSOC had a markedly lower risk of dying

from their disease (HR 0.25, 95% CI 0.06–1.00, p = 0.050), though the p-value remains at the border of significance. The same direction of protective influence was separately tested by two well-established independent software implementations, although the exact point estimates varied due to the different default scales used by each software to determine the strength of the ridge penalty (**Table 4**). Severe frailty and a higher operative burden were also associated with greater risk, although neither reached significance on its own. We then repeated the analysis using any death, not just a cancer-related one, as the outcome (DOD + DOC combined, n=14 events). Under this broader definition, the OSOC effect became weaker (HR 0.60, 95% CI 0.19–1.85, p = 0.372), while frailty (HR 3.70, 95% CI 1.21–11.26, p = 0.022) and operative burden (HR 1.81 per 100-minute increment, 95% CI 1.15–2.86, p = 0.010) became significant predictors instead. This finding closely corresponds to the clinical picture: oncologic clearance primarily protects against dying from the cancer itself, while frailty and total reconstructive burden are general predictors of death from any cause. Therefore, we present the disease-specific model as our main analysis since it isolates the survival advantage of oncologic clearance from the systemic risks of frailty and reconstructive burden, which signifies the central balance point of interest examined in this study.

In the non-NMSC cohort, two atypical Nd cases (Patients #28 and #29) resulted in PTT; 2-cm margins achieved ongoing TFS of 4 and 6 years. Three mNd cases revealed highly aggressive malignancies: Patient 31 (MM, 45-mm Breslow) achieved OSOC and 22-month TFS with adjuvant therapy before fatal acute brain metastasis. Patient 30 (PMC) suffered rapid neck metastasis prior to final pathology and died shortly after, despite prioritizing oncologic clearance over a failed FF. Patient 32 (HAC) underwent aggressive surgery for 6 nodes with extranodal extension but succumbed to distant metastasis within weeks. In Patient #33, clinical suspicion overriding a benign SCAP biopsy prompted a 2-cm resection including periosteum, confirming SCACP; the patient refused ND and adjuvant therapy, leading to rapid mortality. Lastly, a neglected post-traumatic scalp DFSP with bone invasion (Patient #34) required a 4-cm margin resection. Following FF failure, the 251.2 cm^2 defect was successfully salvaged with a rotation flap—necessitating a secondary dog-ear revision—yielding an ongoing TFS of >7 years.

III. Discussion

While frailty has been identified as an important risk factor for early death after major cancer operations[22], its application to skin cancers represents a significant clinical conundrum. Subjecting a frail patient to a major operation for a slowly growing, impossible-to-overlook, giant tumor that they have harbored and perhaps already become accustomed to over the years paradoxically risks triggering early mortality. Overwhelmed by this physiological threat, patients and the healthcare professionals involved in their care may lean toward alternative treatment modalities[23-25] in lieu of the gold standard surgical treatment, or even decide against treatment, often failing to anticipate the devastating consequences of delaying definitive excision. Because neglected NMSC is locally aggressive but rarely metastasizes rapidly, avoiding surgery does not lead to a quick death. Instead, it typically results in a prolonged decline marked by progressive tissue necrosis, chronic suppuration, and severe pain (**Figure 4**). Recent literature rightly cautions that surgery may offer limited survival benefit in frail patients with indolent tumors[10, 11]; on the other hand, withholding surgery exposes the patient to a difficult and prolonged disease course. In another words, proceeding with surgery introduces immediate physical stress whilst withholding it allows the disease to progress unchecked. Consequently, both the patient and the surgeon are therefore left to consider two imperfect options.

This clinical dilemma is clearly reflected in our cohort. A significant majority of patients (88.2%, n=30 of 34) harbored tumors known for indolent yet locally aggressive behavior, specifically SCC (n=21), BCC (n=6), PTT (n=2), and DFSP (n=1). On the one side, however, this low activity of cancer cells has been sharply contrasted with those patients' physical fragility; indeed, approximately fifty percent (n=19) of the population studied exhibited a significant level of frailty as indicated by their mFI-5 score being at least three, while another twenty percent (n=12) were moderately frail, defined by a mFI-5 score equal to two. This discordance between a slow-growing tumor biology and a fragile host helps explain why neglect persisted for so long without fatal consequence in most cases. When applying our six-category model of neglect, it is evident that CD neglect was the dominant type of neglect experienced within this study's population (n=28, 82.4%); next was FR-related neglect (n=5, 14.7%),

and BN (n=1, 2.9%); none of the participants qualified under the categories of Legrand et al.[2], namely: negligence/denial, avoidance, or barrier to access. Furthermore, we would like to make some comments about the predominant role of CD in neglect. Most of the patients in question were dependent on relatives or informal caregivers for recognizing that there was a health problem, seeking help for it, and bringing them into a hospital. Regardless of age, these individuals relied upon someone else to manage the physical burden of traveling to a healthcare facility that specializes in their condition. As has been demonstrated in previous research regarding the burdens experienced by informal caregivers for cancer patients[26], many of these caregivers also experience disproportionate levels of logistical burden. Based on this perspective, we posit that the reliance on caregivers to overcome the logistics associated with accessing care is inextricably linked to other forms of socioeconomic or access-related restrictions. The ability to transport an individual to a healthcare facility, take time away from employment or job responsibilities, or schedule multiple trips to a hospital is all dependent on a family's existing economic and social resources. Therefore, based on our perspective, dependence on caregivers should be viewed as a manifestation of the same barriers to accessing care previously discussed by Legrand et al.[2],but highlighted through the lens of our elderly, co-morbid population.

The literature broadly links prolonged operative time to higher complication rates[27], longer hospital stays[28], and increased mortality[27, 28]. Our data suggest this relationship is not uniform but sharply modulated by baseline frailty. Frail patients experienced a longer duration of hospitalization due to major postoperative complications which necessitated additional interventions. In our sample of severely frail patients (mFi-5 ≥3), those who succumbed to their disease during the study period accumulated on average approximately twice the total amount of cumulative surgery burden compared to the rest of the sample population (mean of 355.0 minutes vs. 171.5 minutes respectively). The impact of surgery burden on outcomes is illustrated in detail with specific examples: Patient #4 (total surgery burden of 590 min.) and Patient #8 (total surgery burden of 410 min.) both rapidly deteriorated despite maximal reconstructive efforts while Patient #26, another equally frail patient (mFi-5 =3) whose reconstruction required a significantly lower surgical burden (cumulative burden of 130 min.), lived for an additional 40 months without cancer recurrence. It should be noted that frailty did not solely

contribute to vulnerability in our sample. Of the three non-frail patients (mFi-5 ≤1) included within our cohort, the two patients (#30 and #32) who quickly expired after undergoing surgery each failed to achieve complete oncologic clearance whereas the third patient (#34) survived for a further 89 months with no evidence of recurrent tumor after complete oncologic clearance and a cumulative burden of 570 min.

Classic reconstructive algorithms, such as those proposed by Iblher et al.[8] and Desai et al.[9], generally reserve local scalp flaps for defects under 30–50 cm², defaulting to free tissue transfer beyond this range. Over our 10-year experience, extended rotation (**Figure 5, 6, 7 and 8**) and regional techniques, Orticochea (**Figure 9**), STAP (**Figure 10**), and trapezius flaps (**Figure 11 and 12**), routinely closed defects well beyond these boundaries, shortening these high-risk procedures. Rotation alone closed a single-stage 163.28 cm² defect (Patient #12, **Figure 7**), consistent with literature supporting expanded rotational limits[29]. Our largest case, a 251.2 cm² defect (Patient #34, **Figure 8**), was closed with a two-stage rotation flap after an initial latissimus dorsi free flap failed. The Orticochea flap[30, 31]—was particularly valuable, offering graftless coverage across the frontal, vertex, and occipital regions well beyond 50 cm², meaningfully shortening reconstructive time in our frail population. Provided a resulting dog-ear deformity or later revision is acceptable, local rotation can be extended well past conventional size limits. This preference was best justified within the overlap zone (62.8–86.35 cm², **Figure 1**), where local, regional, and free flaps were all used: including RD cases, local flaps averaged 191.7 minutes here versus 320.0 minutes for free flaps, a decisive difference for vulnerable patients. We therefore favored extended local or regional rotation over free tissue transfer unless defect location or case-specific factors dictated otherwise. Free tissue transfer remained essential when local/regional options were inadequate (**Figure 13**), when either durable coverage over alloplastic material was required or postoperative radiotherapy was planned (**Figure 14**), or when a two-team approach allowed concurrent resection and reconstruction (**Figure 15**).

Radical resection with negative margins remains a well-established determinant of survival [32-34], including in advanced cutaneous SCC, where a histologic margin of 5 mm or more has been associated with markedly improved disease-specific survival[35]. Achieving this balance is where

surgical experience is most critical: the surgeon must judge resection depth and tissue planes within the complex three-dimensional anatomy of the scalp and calvarium, then reconstruct accordingly, layer by layer. While it is of utmost importance to minimize the length of an operation as much as possible, especially in a highly frail population, it should not compromise the oncologic clearance. This finding directly addresses the tension raised earlier. The risk-benefit balance for surgery in frail patients with early, indolent lesions differs fundamentally from that in patients presenting with neglected, locally advanced disease. In the latter, achieving complete resection appears to outweigh the risks of the procedure itself. Our Cox model supported this directly. Achieving OSOC was associated with a substantially lower risk of disease-specific death (HR 0.25, 95% CI 0.06–1.00), even after adjusting for severe frailty and operative burden; this protective direction held consistently across independent cross-validation (**Table 4**). Compromised resection therefore, carried a correspondingly severe cost. Within the severely frail subgroup, OSOC failure was associated with an 80.0% disease-specific mortality rate and rapid early death. This exposes a vicious cycle[36]. Severe frailty can itself constrain how aggressively a surgeon is willing to operate, and the resulting incomplete clearance then accelerates further physiological decline. This pattern was highly subgroup-specific. Among SCC patients (n=21), OSOC was achieved in 76.2% (16/21), with a mean tumor-free survival of 14.3 months. All five disease-specific deaths in the entire NMSC subgroup occurred within this group, and four of them followed OSOC failure. In contrast, the BCC group (n=6) achieved OSOC in 100% of cases, with zero disease-specific deaths and a mean tumor-free survival of 47.2 months.

Scalp neoplasms that deviate from the classic phenotypes of BCC, SCC, or MM demand a high index of suspicion, especially when they appear deceptively benign or atypical. Initial biopsies of these heterogeneous lesions carry real diagnostic risk. Sampling only a benign component often yields non-definitive results[37, 38]. Our cohort illustrated this pitfall clearly. An initial biopsy reassured the clinical picture as a benign SCAP. Final excision revised this to a malignant SCACP (**Figure 16,** Patient #32), and this delay postponed definitive oncological treatment. Time lost to such diagnostic ambiguity gives the tumor an unforgiving window to progress. This urgency grows even sharper with rare, highly aggressive variants. During the definitive diagnostic workup, both the HAC case (**Figure 17**, Patient

#32) and the PMC case (**Figure 18**, Patient #30) showed rapid local progression and regional spread. Failure to achieve OSOC in these aggressive phenotypes sharply accelerated the terminal course. The MM case (**Figure 19**, Patient #31) showed the opposite pattern. Despite prolonged preoperative neglect, successful OSOC combined with tailored adjuvant therapy allowed a notable 22-month survival. In neglected, atypical scalp masses, an ambiguous or non-diagnostic biopsy can be more dangerous than a confirmed malignancy. It often misguides the surgeon toward an inadequate first resection. Patients #28 and #32 illustrate this risk sharply. Both presented with a firm, fixed, tensely vascularized lesion in the occipital region, phenotypically almost identical. Patient #28's initial biopsy was non-diagnostic (Nd), and the lesion later proved to be PTT, a benign entity. Patient 32's initial biopsy was malignant but non-diagnostic (mNd), and the lesion later proved to be an aggressive malignancy. A malignant-but-non-diagnostic result naturally prompts caution. A simple non-diagnostic result does not, and this is exactly where the danger lies, since it can falsely reassure the surgeon into accepting narrower margins or an incomplete resection. For this reason, we favor treating undiagnosed advanced lesions empirically with wide local excision, using 1.5- to 2-cm margins that include the periosteum. This approach proved decisive. Patients #28 and #29 were ultimately diagnosed with PTT, a tumor known for aggressive behavior and high recurrence risk. These wide margins were still sufficient[39] to achieve a long-term, recurrence-free cure.

Several limitations should be acknowledged. This retrospective, single-center study had a small sample size, limiting generalizability and introducing selection bias. The cohort was inherently heterogeneous in histology, defect size, and reconstructive need, since it was defined by extreme neglect rather than a single diagnosis. Neglect duration relied on patient recall and remains subjective, and the six neglect-type categories were likewise assigned retrospectively, carrying a risk of misclassification. Reconstructive modality was chosen by the surgeon rather than randomized, so our modality comparisons, including **Table 3,** remain descriptive and may reflect indication bias. The ten-year study period also spans real evolution in surgical technique and experience, an unadjusted temporal factor. Our statistical code was custom-written in *Python*. Cross-validation against two independent, established implementations (*Python's lifelines* and *R's survival* package; **Table 4**) confirmed the

direction but not the precise magnitude of the OSOC effect, reflecting known sensitivity of small-sample penalized estimates to software-specific penalty scaling rather than disagreement about the underlying association. Given the limited events, we avoided forcing our data into unsuited parametric models and instead used Fisher's exact test and ridge-penalized Cox regression, both appropriate for small cohorts. Ridge penalization ($\lambda = 1.0$) was necessary because the low events-per-covariate ratio caused the unpenalized model to fail through quasi-complete separation, which also explains the wide confidence interval around the OSOC effect (HR 0.25, 95% CI 0.06–1.00). We modeled disease-specific death as our primary endpoint rather than all-cause mortality, since combining both in a sensitivity analysis shifted significance from OSOC toward frailty and operative burden. This cause-specific approach is not a formal competing-risks model, and future studies with more events should apply subdistribution methods such as Fine-Gray. The non-NMSC subgroup (n=7) was too small and heterogeneous for formal comparison and was reported descriptively only. Given these constraints, our findings should be read as strong observational trends rather than definitive predictive rules, and large-scale, prospective, multi-center studies remain necessary to validate these reconstructive paradigms.

Conclusions

Neglect of large scalp tumors puts elderly patients at risk of three converging factors: advanced tumor burden, physiological vulnerability, and a demanding reconstructive requirement. Our ten-year experience shows that this triad, while risky and formidable, is not unmanageable. Even in our most physiologically vulnerable patients, achieving complete oncological clearance rather than frailty alone emerged as the dominant determinant of disease-specific survival. This finding suggests that curative resection should not be withheld out of excessive caution towards frailty. Instead, it supports a strategy that pairs uncompromising oncological radicality with calculated reconstructive burden reduction. Extending local and regional flap techniques well beyond classic size limits allowed us to shorten high-risk procedures without sacrificing tumor clearance, offering a practical path for surgeons managing similarly frail, complex patients. Strict attention to atypical or non-diagnostic biopsies further proved essential, since diagnostic delay compounds the risks already posed by neglect and frailty. Taken together, our findings suggest that even the most extensively neglected scalp malignancies in the frailest patients can be approached with curative intent, provided that reconstructive strategy is carefully tailored to minimize operative burden. Larger, prospective, multi-center studies are needed to confirm and refine this approach.

Declarations

Abbreviations

AJCC: American Joint Committee on Cancer

ALT: Anterolateral thigh

ASA: American Society of Anesthesiologists Physical Status Classification System

BCC: Basal cell carcinoma

BN: Banalization

CD: Caregiver-dependent

CHF: Congestive heart failure

CHT: Chemotherapy

CI: Confidence interval

COPD: Chronic obstructive pulmonary disease

DFSP: Dermatofibrosarcoma protuberans

DM: Diabetes mellitus

DMe: Distant metastasis

DOC: Dead of other causes

DOD: Dead of disease

ENE: Extranodal extension

FF: Free flap

HAC: Hidradenocarcinoma

HR: Hazard ratio

HT: Hypertension

ICU: Intensive care unit

IT: Immunotherapy

LD: Latissimus dorsi

LF: Local flap

LN: Lymph node

LR: Local recurrence

LTFU: Lost to follow-up

mFI-5: Modified Frailty Index-5

MI: Myocardial infarction

MM: Malignant melanoma

mNd: Malignant but non-definitive diagnosis

NCCN: National Comprehensive Cancer Network

Nd: Non-diagnostic

NM: Nodal metastasis

NMSC: Non-melanoma skin cancer

OSOC: Overall surgical oncologic clearance

PMC: Pilomatrixal carcinoma

PMMA: Polymethyl methacrylate

PTT: Proliferating trichilemmal tumor

RD: Regional dissection (neck dissection ± parotidectomy)

RF: Regional flap

RT: Radiotherapy

SCAP: Syringocystadenoma papilliferum

SCACP: Syringocystadenocarcinoma papilliferum

SCC: Squamous cell carcinoma

SD: Standard deviation

STAP: Superficial temporal artery perforator

STSG: Split-thickness skin graft

TFS: Tumor-free survival

VC: Venous congestion

XP: Xeroderma pigmentosum

Ethics Approval and Consent to Participate

This study was approved by the Clinical Research Ethics Committee of the University of Health Sciences, Şişli Hamidiye Etfal Training and Research Hospital (approval number: 5589/2026). The study was conducted in accordance with the principles of the Declaration of Helsinki. Written informed consent to participate in the study was obtained from all participants or their legal guardians, where applicable.

Consent for publication

Written informed consent for publication of the participants' personal and clinical details and any identifying clinical images was obtained from all participants or their legal guardians, where

applicable. This consent explicitly included permission to publish unmasked identifying images. For participants who were deceased at the time of publication, written informed consent for publication was also obtained from their next of kin.

Availability of data and materials

The dataset and custom *Python* code used for statistical analysis in this study are available at:

https://github.com/ofdilek-design/scalp-reconstruction-cox-model-

Competing interests

The authors declare that they have no competing interests.

Funding

This research received no specific grant from any funding agency in the public, commercial, or not-for-profit sectors.

Authors' contributions

Ö.F.D. conceived and designed the study, performed the surgical procedures, conducted the statistical analysis, and drafted the manuscript. S.B. performed the surgical procedures and contributed to the study design. M.D.Ç. and Y.A. contributed to data collection, patient follow-up, and coordination of clinical records. B.B. performed the histopathological evaluation and interpretation of all specimens. S.H.A. supervised the study and critically revised the manuscript for important intellectual content. K.Z.S. performed the surgical procedures and supervised the study, critically revising the manuscript for important intellectual content. All authors read and approved the final manuscript.

Acknowledgements

Not applicable.

Figure Legends

Figure 1

Relationship between defect size and reconstructive modality across the full cohort (n=34). Defects below 62.8 cm² were predominantly closed with local flaps (LF, 12/13, 92.3%). An overlap zone between 62.8 and 86.35 cm² (n=12) permitted local (LF, n=6), regional (RF, n=4), and free flap (FF, n=2) reconstruction. Defects above 86.35 cm² were predominantly closed with free flaps (FF, 5/9, 55.6%), with local flaps used for the remainder (4/9, 44.4%) and no regional flaps in this range. LF, local flap; RF, regional flap; FF, free flap

Figure 2

Association between total cumulative operative burden and overall survival, stratified by frailty and oncological clearance status. Each point represents one patient, plotted by total operative burden (x-axis, minutes) against overall survival (y-axis, months; not tumor-free survival). The NMSC cohort (Patients 1–27) is plotted above the central reference line, and the non-NMSC cohort (Patients 28–34) is plotted below it in mirrored fashion for visual separation; distance from the central line in either direction reflects survival duration in months. Marker shape denotes oncological clearance status, with circles indicating achieved OSOC and squares indicating failed OSOC. Marker color denotes frailty severity (mFI-5), with green representing robust patients (mFI-5 0–1), orange representing moderate frailty (mFI-5 = 2), and red representing severe frailty (mFI-5 ≥3). A black cross denotes disease-specific death (DOD) and a blue cross denotes death from other causes (DOC); markers without a cross indicate patients alive at last follow-up. Dashed lines mark the 6-month threshold used to define early postoperative mortality.

Figure 3

Distribution of clinical outcomes among NMSC patients (n=27), stratified by frailty severity and oncological clearance status. Outcomes are shown as the proportion of patients who died of disease (DOD, red), died of other causes (DOC, orange), or remained alive at last follow-up (green). All severely frail patients (mFI-5 ≥3) who failed to achieve OSOC (n=5) had the poorest outcomes, with 80.0% disease-specific mortality. Among severely frail patients who achieved OSOC (n=11), disease-specific mortality fell to 9.1%, though 54.5% died of other causes. Moderately frail patients (mFI-5 = 2, n=11) uniformly achieved OSOC, with no disease-specific deaths and 72.7% alive at last follow-up.

Figure 4

These four cases illustrate how agonizing and dramatic the disease course can become once the surgical window has closed. All patients were operable years earlier at initial presentation but did not undergo resection, instead receiving no treatment or alternative treatment modalities. Panels A and C show squamous cell carcinoma (SCC) in the terminal stage, within the final month of life. Panels B and D show basal cell carcinoma (BCC), with both patients surviving at least six months beyond this stage without surgical intervention.

Figure 5

Reconstructive course of patient 1, an 83-year-old woman with a parietooccipital squamous cell carcinoma neglected for more than two years. (A, B) Preoperative views show a large, ulcerated, exudative scalp tumor with extensive crusting and necrotic slough, reflecting the prolonged period of neglect. (C) Intraoperative view after wide local excision, showing the resulting full-thickness scalp defect (94.98 cm^2) with the pericranium exposed. (D) A large rotation flap is elevated and advanced to cover the defect. (E, F) Postoperative follow-up views show a well-healed, stable reconstruction with satisfactory contour and hair-bearing coverage.

The patient achieved oncological clearance and remained tumor-free until her death from an unrelated asthma attack at 23 months postoperatively.

Figure 6

Surgical and clinical course of a giant left frontotemporal tumor (Patient 11). (A) Preoperative presentation of a massive, exophytic, and fungating mass on the left frontotemporal scalp. (B) Intraoperative marking for wide local excision; notably, there was no macroscopic or radiological evidence of cranial bone invasion. (C, D) Postoperative frontal and lateral views demonstrating defect reconstruction with a large rotation flap, combined with split-thickness skin grafting of the secondary donor site. Due to high-risk histopathological features, including a 9-mm depth of invasion, the patient subsequently underwent an elective superficial parotidectomy and neck dissection. The patient expired due to pulmonary failure at the 10th postoperative month. No local recurrence or distant metastasis was detected during the follow-up period.

Figure 7

Surgical management and clinical evolution of a neglected scalp neoplasm in a high-frailty patient (Patient 12; 78 years old, mFI-5 score = 4). (A) Preoperative view of a long-standing (>4 years) fronto-scalp lesion. (B) Intraoperative assessment showing calvarial and frontal sinus invasion. (C) Defect after composite bone and dural resection. (D, E) Stable postoperative outcome at 3 weeks following rotation flap reconstruction. (F) Status at postoperative month 20 following a re-excision at month 14 for a 2-cm recurrence. The patient subsequently developed a repeat recurrence at the surgical site and has refused further oncological or surgical intervention.

Figure 8

Staged reconstructive course of patient 34 (defect size 251.2 cm^2), illustrating both the consequences of prolonged neglect and the complexity of salvage reconstruction. (A) Occipital lesion at the site of a childhood trauma, neglected for more than four years before presentation. (B) Intraoperative view following resection with 4 cm margins, including the underlying cortical bone given radiologic evidence of bone invasion, followed by immediate titanium mesh cranioplasty. (C) Coverage of the mesh with a free latissimus dorsi myocutaneous flap. (D) The flap subsequently failed due to a venous vascular event, a significant early setback in the reconstructive course. (E) Salvage reconstruction was achieved with a large rotation flap, at the cost of a prominent dog-ear deformity, with the resulting donor defect closed by a split-thickness skin graft. (F, G) Lateral and frontal views after this first salvage stage show a stable, healed result despite the residual aesthetic compromise. (H, I) A second-stage revision used the dog-ear tissue more efficiently, reducing the grafted surface area and improving overall contour. (J) Final lateral view showing the definitive outcome. This sequence illustrates how a single vascular complication can turn a straightforward reconstruction into a multistage salvage effort, and how iterative revision can still recover an acceptable result.

Figure 9

Reconstructive course of patient 2, a 78-year-old woman with a vertex squamous cell carcinoma neglected for 26 months. (A) Preoperative view showing a crusted, ulcerated tumor with extensive yellow slough at the vertex. (B) Intraoperative view after wide local excision, showing the resulting full-thickness scalp defect with the pericranium exposed and resection margins marked. (C) The classic three-flap Orticochea design is elevated, mobilizing scalp tissue from three directions around the defect. (D) The flaps are rotated and advanced into a triradiate closure, achieving graftless coverage of the defect. (E, F) Postoperative follow-up views show excellent hair-bearing coverage with a well-camouflaged scar pattern. The patient

achieved oncological clearance and remained alive, with 39 months of tumor-free survival at last follow-up.

Figure 10

Reconstructive course and eventual disease progression in patient 9, a 93-year-old woman with a frontal SCC neglected for 20 months. (A) Preoperative view showing a round, exophytic, keratotic tumor nodule. (B) Intraoperative view after wide local excision, showing the resulting full-thickness scalp defect with the pericranium exposed. (C) Postoperative view showing stable coverage achieved with a superficial temporal artery perforator (STAP) flap. (D) Local recurrence with distant metastasis, leading to disease-specific death at 15 months. This patient is the only case in our cohort of a sudden, rapidly progressive recurrence despite achieved OSOC and histopathology free of adverse prognostic features, underscoring that frailty alone can still drive a fatal outcome in an otherwise favorable neglected tumor.

Figure 11

Reconstructive course of patient 28, a 79-year-old woman with an occipital scalp lesion neglected for more than four years. (A) Preoperative view showing a relatively subtle, firm subcutaneous nodule beneath the hairline, deceptively unremarkable despite its long neglect. (B) Intraoperative view after wide local excision, performed empirically given a non-diagnostic initial biopsy, showing the resulting defect with a residual firm nodular component in the wound bed. (C) A trapezius myocutaneous flap is elevated and rotated toward the defect. (D) Postoperative view shows a well-healed, aesthetically favorable result. The lesion was ultimately confirmed as a proliferating trichilemmal tumor (PTT), an entity notorious for local aggressiveness and a high propensity for recurrence despite its typically benign histology. The

empirical 2 cm prophylactic margin proved sufficient to prevent recurrence, and the patient remained tumor-free for 51 months.

Figure 12

Reconstructive course of patient 25, a 68-year-old man with an occipital basal cell carcinoma neglected for more than six years. (A) Preoperative lateral view showing a large, multilobulated, cauliflower-like exophytic mass at the occipital region. (B) Intraoperative view showing the resected specimen and the trapezius flap donor site marked on the upper back. (C, D) Postoperative views at 3 months show a well-healed reconstruction with good contour at the recipient site and an acceptable linear donor scar on the back. The patient achieved oncological clearance and remained tumor-free for 36 months.

Figure 13

Reconstructive evolution and fatal clinical course of a long-standing scalp SCC in a high-frailty patient (Patient 4; mFI-5 score = 4). (A) Preoperative view of a >10-year neglected, ulcerated SCC lesion, complicated by a concurrent chronic subdural hematoma and suspicious bilateral Level V cervical lymphadenopathy (up to 1.5 cm). (B) Defect following radical tumor extirpation, concurrent bilateral neck dissection, and calvarial burring, initially managed with a temporary wound matrix to prepare the bed for a split-thickness skin graft. (C) Widespread suppurative infection throughout the entire temporary matrix at postoperative day 5. (D) Inadequate granulation tissue formation despite targeted wound care, prompting a rescue conversion to a free latissimus dorsi muscle flap. (E) Microvascular recipient site assessment revealing a densely calcified superficial temporal artery and a highly fragile superficial temporal vein (inferior). (F) Final reconstruction following LD flap inset. The patient experienced an arterial vascular crisis requiring re-exploration at 36 hours and subsequently

succumbed to the cumulative physiological stress in the intensive care unit on postoperative day 5.

Figure 14

Reconstructive course of patient 5, a 61-year-old man with a parietovertex SCC neglected for 14 months. (A) Preoperative view showing an exophytic nodular tumor with the planned resection margins marked. (B) Intraoperative view after skin incision and tumor exposure down to the calvarium. (C) Bone resection reveals dural invasion at the tumor base. (D) Duraplasty is performed using a fascia lata graft. (E) The cranial defect is reconstructed with a titanium mesh. (F) A free anterolateral thigh (ALT) flap is inset and sutured to provide durable soft-tissue coverage. (G, H) Postoperative views at 3 months show a well-healed reconstruction with stable contour and satisfactory hair-bearing coverage at the margins. The patient received adjuvant radiotherapy and remained alive, with 13 months of tumor-free survival at last follow-up.

Figure 15

Reconstructive course of patient 24. (A) Preoperative view of a 37-year-old patient (mFI-5 score = 2) presenting with an extensive frontal BCC neglected for >5 years. (B) Full-thickness defect following wide radical oncological resection exposing calvarial bone. (C) Postoperative outcome at month 3 showing stable, vascularized soft-tissue coverage achieved via an immediate free anterolateral thigh (ALT) flap. (D) 7 years post-surgery, demonstrates durable soft-tissue contouring without local recurrence.

Figure 16

Clinical and histopathological course of patient 33. (A) Preoperative view of a massive, atypical scalp lesion with a history of neglect for over 5 years. (B, C) Initial incisional biopsy revealing benign SCAP with orderly papillary structures projecting into cystic spaces and no

cellular atypia (H&E; ×2 for B, ×4 for C). (D) Due to the prolonged history and atypical appearance, a wide local excision with 2 cm margins was performed, and the defect was reconstructed with a pedicled lower trapezius flap. Distal flap necrosis developed (E) and was subsequently managed with debridement and a split-thickness skin graft (F). Complete healing was achieved by the second postoperative month (G). (H, I) Final pathology of the excision specimen revealed malignant transformation to SCACP, with high-power fields showing complete loss of papillary architecture, severe cellular pleomorphism, high-grade atypia, and bizarre multinucleated giant cells (H&E; ×10 for H, ×15.8 for I). Immunohistochemistry performed on these pleomorphic cells showed positive staining for p40, CK5/6, CK7, and pan-cytokeratin, confirming their squamous epithelial origin. (J) The patient refused all recommendations for regional dissection and adjuvant therapy, developing a massive regional neck metastasis at the 6th postoperative month, and continued to decline further intervention, dying at the 9th postoperative month

Figure 17

Clinical and histopathological course of patient 32. (A) Preoperative view of a 1-year neglected suboccipital mass with palpable regional lymphadenopathy in a 49-year-old female, managed via wide resection, posterolateral neck dissection, and pedicled trapezius flap reconstruction. (B) Infiltrative multinodular architecture composed of dermal epithelial lobules extending into the subcutis (17.8×, H&E). (D) Biphasic cellular proliferation comprising clear and eosinophilic cells with focal necrosis (6.6×, H&E). (C) Marked cytological atypia, nuclear pleomorphism, brisk mitoses, and neurovascular invasion establishing the definitive diagnosis of high-grade hidradenocarcinoma (HAC) (6×, H&E). Immunohistochemistry supported this diagnosis, with tumor cells staining positive for S100 and EMA, and negative for m-CEA, PAX-8, TTF-1, and thyroglobulin, excluding thyroid, salivary, and other adnexal mimickers. The Ki-67 proliferation index reached 60% in hotspot areas, reflecting the tumor's high-grade,

aggressive biology. Fulminant locoregional recurrence developed at postoperative month 2, and the patient died 4 months after surgery.

Figure 18

Clinical course of patient 30, a 38-year-old woman with an occipital scalp tumor, ultimately confirmed as pilomatrixal carcinoma (PMC), neglected for 19 months. (A) Preoperative view of the lesion at initial presentation. (B) Reconstruction with PMMA cranioplasty following bone resection; the free latissimus dorsi flap used for soft-tissue coverage subsequently failed due to venous insufficiency. Following this failure, definitive reconstruction was deliberately delayed until final histopathology was available, so that all remaining necessary procedures could be consolidated into a single session. At 4 weeks, once PMC was confirmed, the inferior resection margin was widened together with a neck dissection. (C) The resulting defect was then reconstructed with local flaps. (D) At 7 weeks, the local flap reconstruction was only partially successful. Histopathology reported widespread margin positivity, and clinically there was overt recurrence at the inferior margin. Adjuvant therapy was rapidly initiated, but the patient died at postoperative week 11 with multiple distant metastases present. (E, F) Histopathology showed, beneath an intact epidermis, a full-thickness infiltrative basaloid tumor arising in a fibromyxoid stroma, with extensive desmoplasia, necrosis, focal keratinization, marked pleomorphism, hyperchromasia, prominent eosinophilic nucleoli, atypical mitoses (up to 18 per 10 high-power fields in the recurrence specimen), and focal cytoplasmic clearing. Lymphovascular invasion was present, perineural invasion was absent, and the deep bone margin was free of tumor at the primary resection. Immunohistochemistry showed diffuse, though mild, β-catenin positivity within tumor cells, supporting the diagnosis, while CD34 highlighted the invaded vessels. Mismatch repair proteins (MSH2, MSH6, MLH1, PMS2) showed retained nuclear expression, and CD117 was negative, arguing against a mismatch-repair-deficient or KIT-driven process.

Figure 19

Clinical and histopathological course of patient 31. (A) Preoperative view of a 1.5-year neglected, massive exophytic scalp tumor with surface ulceration. (B) Defect following wide oncological resection and concurrent posterolateral neck dissection for palpable nodal disease. (C) Postoperative day 10 view showing stable reconstruction via a rotation flap. (D, E) Low- (1.1×, H&E) and high-power (20.6×, H&E) histopathology confirming an exceptionally aggressive nodular MM composed of pleomorphic spindle/epithelioid cells, reaching a remarkable 45 mm Breslow depth of invasion. Immunohistochemistry showed tumor cells positive for S100, while HMB45 and Melan-A, each repeated three times to exclude a technical false negative, remained negative, along with CD34, CEA, ERG, pan-cytokeratin, and p16, a profile consistent with a poorly differentiated, dedifferentiated melanoma in which classic melanocytic markers are lost while S100 positivity and exclusion of vascular, epithelial, and other mesenchymal mimickers support the diagnosis. Despite maintaining locoregional control for 22 months post-adjuvant therapy, the patient subsequently developed fatal cerebral metastasis and died 4 months later.

Tables

Table 1. Patient demographics, clinical characteristics, reconstructive procedures, and surgical outcomes of the cohort

Patient demographics, clinical characteristics, reconstructive procedures, and surgical outcomes of the cohort. (ALT: Anterolateral thigh; ASA: American Society of Anesthesiologists physical status classification system; AV: Avoidance; BCC: Basal cell carcinoma; BL: Bilateral; BN: Banalization; COPD: Chronic obstructive pulmonary disease; CD: Care Giver-Dependent; CP: Cerebral palsy; CHT: Chemotherapy; d: day; DFSP: Dermatofibrosarcoma protuberans; DM: Diabetes Mellitus; DMe: Distant metastasis; DN: Denial; DOC: Died of other causes; DOD: Died of disease; F: Female; FR: Fear; HAC: Hidradenocarcinoma; HF: Heart failure; HT: Hypertension; ICU: Intensive care unit; IT: Immunotherapy; LD: Latissimus dorsi; LR: Local recurrence; LTFU: Lost to follow-up; M: Male; m: month; mFI-5: modified Frailty Index-5; MI: Myocardial infarction; MM: Malignant melanoma; mNd: Malignant but not definitive; MR: Mental retardation; Nd: Not definitive; RD: Regional Dissection (Neck ± parotid); NM: Nodal metastasis; PMC: Pleomorphic malignant carcinoma; PMMA: Polymethyl methacrylate; PO: Postoperative; pod: Postoperative day; pom: Postoperative month; pow: Postoperative week; poy: Postoperative year; PTT: Proliferating trichilemmal tumor; RA: Rheumatoid arthritis; RT: Radiotherapy; SCACP: Syringocystadenocarcinoma papilliferum; SCAP: Syringocystadenoma papilliferum; SCC: Squamous cell carcinoma; STAP: Superficial temporal artery perforator; STSG: Split-thickness skin graft; TFS: Tumor free survival. TFS was set to 0.1 for statistical purposes when true tumor-free survival was effectively zero: either because macroscopic or microscopic tumor persisted without further adjuvant therapy, or because the patient died in the immediate postoperative period before recurrence status could be meaningfully assessed; UL: Unilateral; VC: Venous congestion; XP: Xeroderma pigmentosa; y: year)

Table 2. Histopathological diagnoses and tumor characteristics of the study cohort.

Detailed histopathological characteristics, surgical margin assessments, high-risk features, and oncological staging of the neglected giant scalp neoplasm cohort. (BCC: Basal cell carcinoma; DFSP: Dermatofibrosarcoma protuberans; ENE: Extranodal extension; HAC: Hidradenocarcinoma; LN: Lymph node; MM: Malignant melanoma; ns: Not specified; PMC: Pleomorphic malignant carcinoma; PTT: Proliferating trichilemmal tumor; SCACP: Syringocystadenocarcinoma papilliferum; SCC: Squamous cell carcinoma)

Table 3. Operative time, hospital stay, and complication rates by reconstructive modality and regional dissection (RD) status (n=34)

Operative time, hospital stay, and major complications by reconstructive modality (LF: local flap; RF: regional/trapezius flap; FF: free flap) and RD status, full cohort (n=34). Operative time excludes complication-related secondary procedures.

Table 4. Cross-validation of the ridge-penalized Cox model for OSOC across independent software implementations (NMSC subgroup, n=27, 5 events)

All three models included OSOC, mFI-5, and cumulative operative burden as covariates. Point estimates vary because each package scales the ridge penalty term differently; the consistent direction of effect (HR < 1) across all three independent implementations supports a genuine protective association between OSOC and disease-specific survival, though the precise magnitude should not be over-interpreted given the small number of events

References

1. Renzi C, Mastroeni S, Mannooranparampil TJ, Passarelli F, Caggiati A, Potenza C, Pasquini P: Delay in diagnosis and treatment of squamous cell carcinoma of the skin. Acta Derm Venereol 2010, 90:595–601.

2. Legrand A, Quintard B, Garrouteigt C, Beylot-Barry M, Broc G: From neglect to earlier diagnosis: a qualitative meta-synthesis of psycho-social factors associated with consultation delay in advanced basal cell carcinoma. Psychol Health Med 2022, 27:1793–1804.

3. Varga E, Korom I, Rasko Z, Kis E, Varga J, Olah J, Kemeny L: Neglected Basal cell carcinomas in the 21st century. J Skin Cancer 2011, 2011:392151.

4. Archontaki M, Stavrianos SD, Korkolis DP, Arnogiannaki N, Vassiliadis V, Liapakis IE, Christ H, Rapidis AD, Kokkalis G: Giant Basal cell carcinoma: clinicopathological analysis of 51 cases and review of the literature. Anticancer Res 2009, 29:2655–2663.

5. Mateuszczyk MK, Chlebicka I, Łyko M, Maj J, Szepietowski JC: Extra-Anogenital Giant Cutaneous Squamous Cell Carcinomas. Life (Basel) 2024, 14.

6. Block LM, Jee YM, Baskaya MK, Bentz ML, Poore SO: Denying the Obvious: Four Extreme Cases of Neglected Tumors. Plast Reconstr Surg Glob Open 2015, 3:e571.

7. Alam M, Goldberg LH, Silapunt S, Gardner ES, Strom SS, Rademaker AW, Margolis DJ: Delayed treatment and continued growth of nonmelanoma skin cancer. J Am Acad Dermatol 2011, 64:839–848.

8. Iblher N, Ziegler MC, Penna V, Eisenhardt SU, Stark GB, Bannasch H: An algorithm for oncologic scalp reconstruction. Plast Reconstr Surg 2010, 126:450–459.

9. Desai SC, Sand JP, Sharon JD, Branham G, Nussenbaum B: Scalp reconstruction: an algorithmic approach and systematic review. JAMA Facial Plast Surg 2015, 17:56–66.

10. Chicco M, Borsky K, Goodall R, Harrison C, Rodrigues J: Outcomes of skin cancer excision in frail patients: A retrospective cohort study. J Plast Reconstr Aesthet Surg 2023, 84:32–36.

11. Thakker S, Minkis K, Lipner SR, Gulati N, Patel VA, Al-Mondhiry J: An ethical framework for managing neglected skin tumors in older patients. J Am Acad Dermatol 2026, 94:395–396.

12. Goshtasbi K, Birkenbeuel JL, Lehrich BM, Abiri A, Haidar YM, Tjoa T, Kuan EC: Association Between 5-Item Modified Frailty Index and Short-term Outcomes in Complex Head and Neck Surgery. Otolaryngol Head Neck Surg 2022, 166:482–489.

13. Subramaniam S, Smith RW, Tanna N, Smith ML: Assessing Frailty in Plastic Surgery: Analysis of the Five-factor Index. Plast Surg (Oakv) 2025, 33:479–483.

14. Nakamura K, Tsukasaki M, Tsunematsu T, Yan M, Ando Y, Huynh NC, Hashimoto K, Gou Q, Muro R, Itabashi A, et al: The periosteum provides a stromal defence against cancer invasion into the bone. Nature 2024, 634:474–481.

15. Tsukasaki M: Dive into the bone: new insights into molecular mechanisms of cancer bone invasion. Journal of Bone and Mineral Research 2025, 40:827–833.

16. Carter RL, Tanner NS, Clifford P, Shaw HJ: Direct bone invasion in squamous carcinomas of the head and neck: pathological and clinical implications. Clin Otolaryngol Allied Sci 1980, 5:107–116.

17. Brown JS, Browne RM: Factors influencing the patterns of invasion of the mandible by oral squamous cell carcinoma. Int J Oral Maxillofac Surg 1995, 24:417–426.

18. Brown JS, Lowe D, Kalavrezos N, D'Souza J, Magennis P, Woolgar J: Patterns of invasion and routes of tumor entry into the mandible by oral squamous cell carcinoma. Head Neck 2002, 24:370–383.

19. Baratz HQ, Schmidtman DC, Yin LX, Moore EJ, Tasche KK, Van Abel KM, Price DL: Impact of Calvarial Burring in Squamous Cell Carcinoma of the Scalp Without Gross Calvarial Involvement. Annals of Otology, Rhinology & Laryngology 2026, 135:530–534.

20. Leach GA, Pflibsen LR, Mathew DP, Sharma AD, Reid CM, Holcombe TC: The Role of Resection of the Outer Table of the Cranium in Locally Invasive Primary Squamous Cell Carcinoma of the Scalp. Journal of Craniofacial Surgery 2022, 33:1860–1864.

21. Leow JJL, Fleming JJF, Oakley RRO: A case series on the conservative management of the bony skull in patients with aggressive skin carcinomas of the scalp. J Surg Case Rep 2018, 2018:rjy326.

22. Dumludağ A, Öcal D, Torun M: Frailty as a determinant of surgical morbidity, adjuvant therapy feasibility, and survival in octogenarian patients undergoing gastrointestinal cancer resection. BMC Geriatrics 2026, 26:392.

23. Kreinbrink PJ, Mierzwa ML, Huth B, Redmond KP, Wise-Draper TM, Casper K, Li J, Takiar V: Adjuvant radiation and cetuximab improves local control in head and neck cutaneous squamous cell carcinoma: Phase II study. Head Neck 2021, 43:3408–3416.

24. Yosefof E, Kurman N, Yaniv D: The Role of Radiation Therapy in the Treatment of Non-Melanoma Skin Cancer. Cancers 2023, 15:2408.

25. Rossi R, Campolmi P, Giomi B, Massi D, Cappugi P: Giant exophytic basal cell carcinoma treated with radiotherapy. Journal of the European Academy of Dermatology and Venereology 2002, 16:374–376.

26. Thomson MD, Van Houtven CH, Xu R, Siminoff LA: The many "costs" of transportation: Examining what cancer caregivers experience as transportation obstacles. Cancer Med 2023, 12:17356–17364.

27. Shahrokni A, Tin AL, Sarraf S, Alexander K, Sun S, Kim SJ, McMillan S, Yulico H, Amirnia F, Downey RJ, et al: Association of Geriatric Comanagement and 90-Day Postoperative Mortality Among Patients Aged 75 Years and Older With Cancer. JAMA Netw Open 2020, 3:e209265.

28. Leung JM, Dzankic S: Relative importance of preoperative health status versus intraoperative factors in predicting postoperative adverse outcomes in geriatric surgical patients. J Am Geriatr Soc 2001, 49:1080–1085.

29. Seretis K, Bounas N, Lykoudis EG: Reconstruction of Scalp Defects with Rotational Flaps: Where Is the Limit? Surgeries 2025, 6.

30. Orticochea M: Four flap scalp reconstruction technique. Br J Plast Surg 1967, 20:159–171.

31. Orticochea M: New three-flap scalp reconstruction technique. British Journal of Plastic Surgery 1971, 24:184–188.

32. Fang Q, Yuan J, Zhang X, Dai L, Luo R: Lymph node metastasis in cutaneous squamous cell carcinoma of the head and neck. BMC Cancer 2024, 24:656.

33. Dessinioti C, Stratigos AJ: Recent Advances in the Diagnosis and Management of High-Risk Cutaneous Squamous Cell Carcinoma. Cancers 2022, 14:3556.

34. Dhiwakar M, Khan NA, McClymont LG: Surgery for head and neck skin tumors in the elderly. Head & Neck 2007, 29:851–856.

35. Phillips TJ, Harris BN, Moore MG, Farwell DG, Bewley AF: Pathological margins and advanced cutaneous squamous cell carcinoma of the head and neck. J Otolaryngol Head Neck Surg 2019, 48:55.

36. Hernández-Aguiar Y, Becerra-Bolaños Á, Rodríguez-Pérez A: Frailty and Oncology: An Increasingly Common Combination. Cancer Med 2026, 15:e71499.

37. Leeborg N, Thompson M, Rossmiller S, Gross N, White C, Gatter K: Diagnostic pitfalls in syringocystadenocarcinoma papilliferum: case report and review of the literature. Arch Pathol Lab Med 2010, 134:1205–1209.

38. Agarwal A, Agarwal P, Anand A, Sagar M, Bhalla S, Agrawal M, Sonkar AA, Goel MM: Nodular Hidradenocarcinoma, Trichelemmal Carcinoma and Squamous Cell Carcinoma with Clear

Cell Changes: Pitfalls of Biopsy Diagnosis of Skin and Adnexal Tumours. Clin Pathol 2021, 14:2632010x211033840.

39. Choi MS, Kim EJ, Lee JH, Pyo JY, Park YW, Lee KM: Scalp reconstruction after resection of a large recurred proliferating trichilemmal tumor using an anterolateral thigh free flap. Arch Plast Surg 2013, 40:458–460.

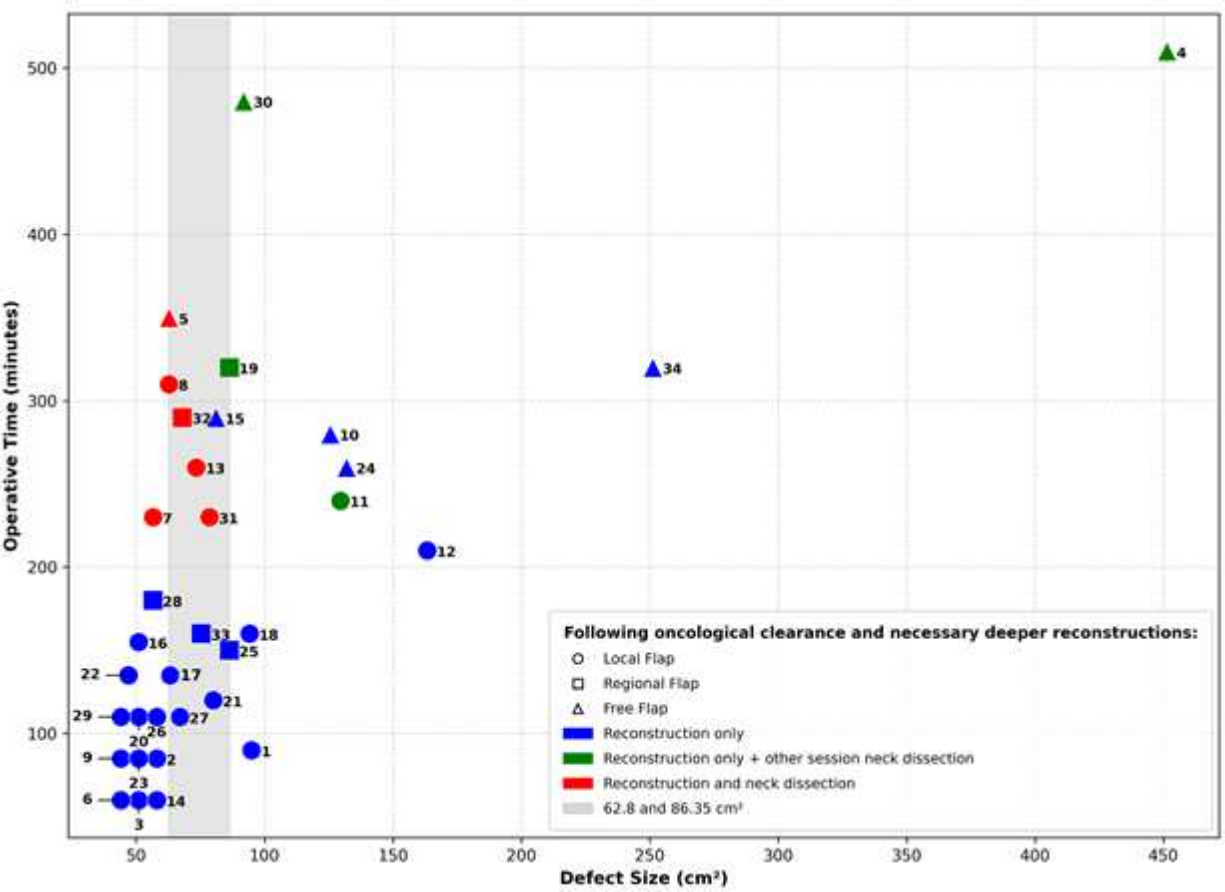
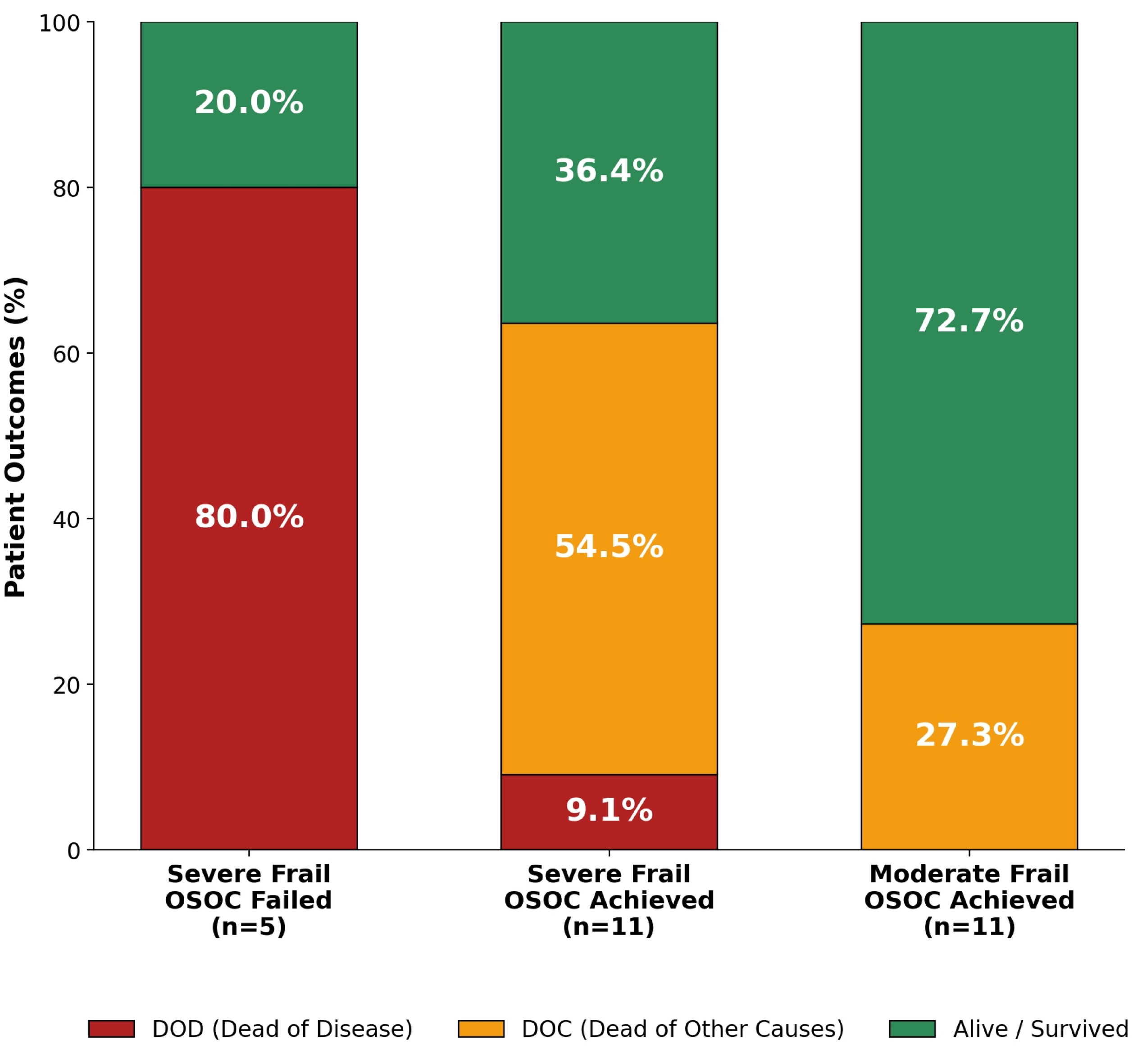

Operative Time (minutes)
Defect Size (cm²)
Following oncological clearance and necessary deeper reconstructions:
Local Flap
Regional Flap
Free Flap
Reconstruction only
Reconstruction only + other session neck dissection
Reconstruction and neck dissection
62.8 and 86.35 cm²

Image not available with this version


Patient Outcomes (%)
100
80
60
40
20
0
20.0%
80.0%
36.4%
54.5%
9.1%
72.7%
27.3%
Severe Frail
OSOC Failed
(n=5)
Severe Frail
OSOC Achieved
(n=11)
Moderate Frail
OSOC Achieved
(n=11)
DOD (Dead of Disease)
DOC (Dead of Other Causes)
Alive / Survived

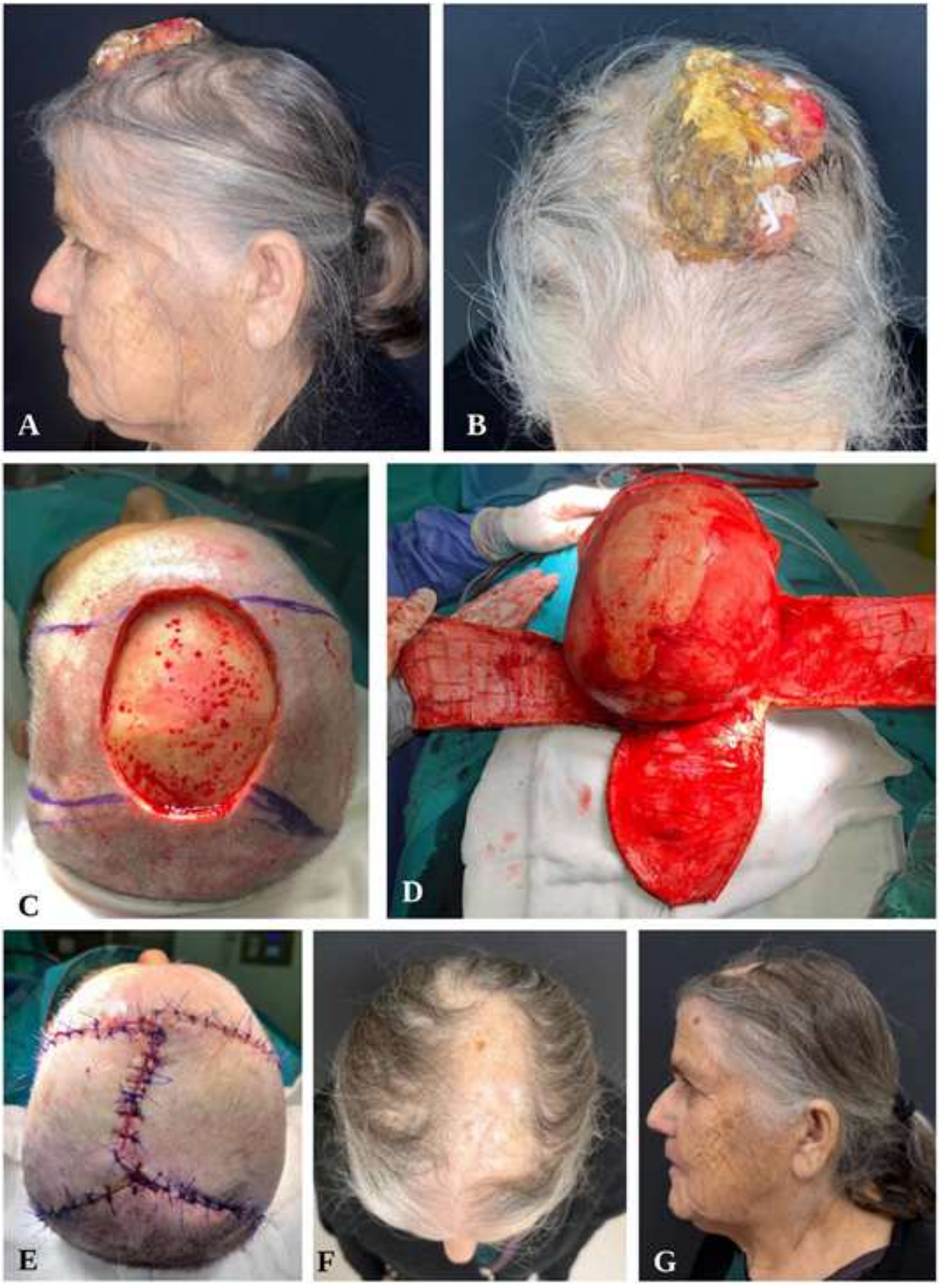

B
C
D


A
B
C
D
E
F


A
B
C
D


A
B
C
D
E
F


A
B
C
D
E
F
G
H
I
J


A
B
C
D
E
F
G


A
B
C
D


A


B


C


D


A
B
C
D


A
B
C
D
E
F





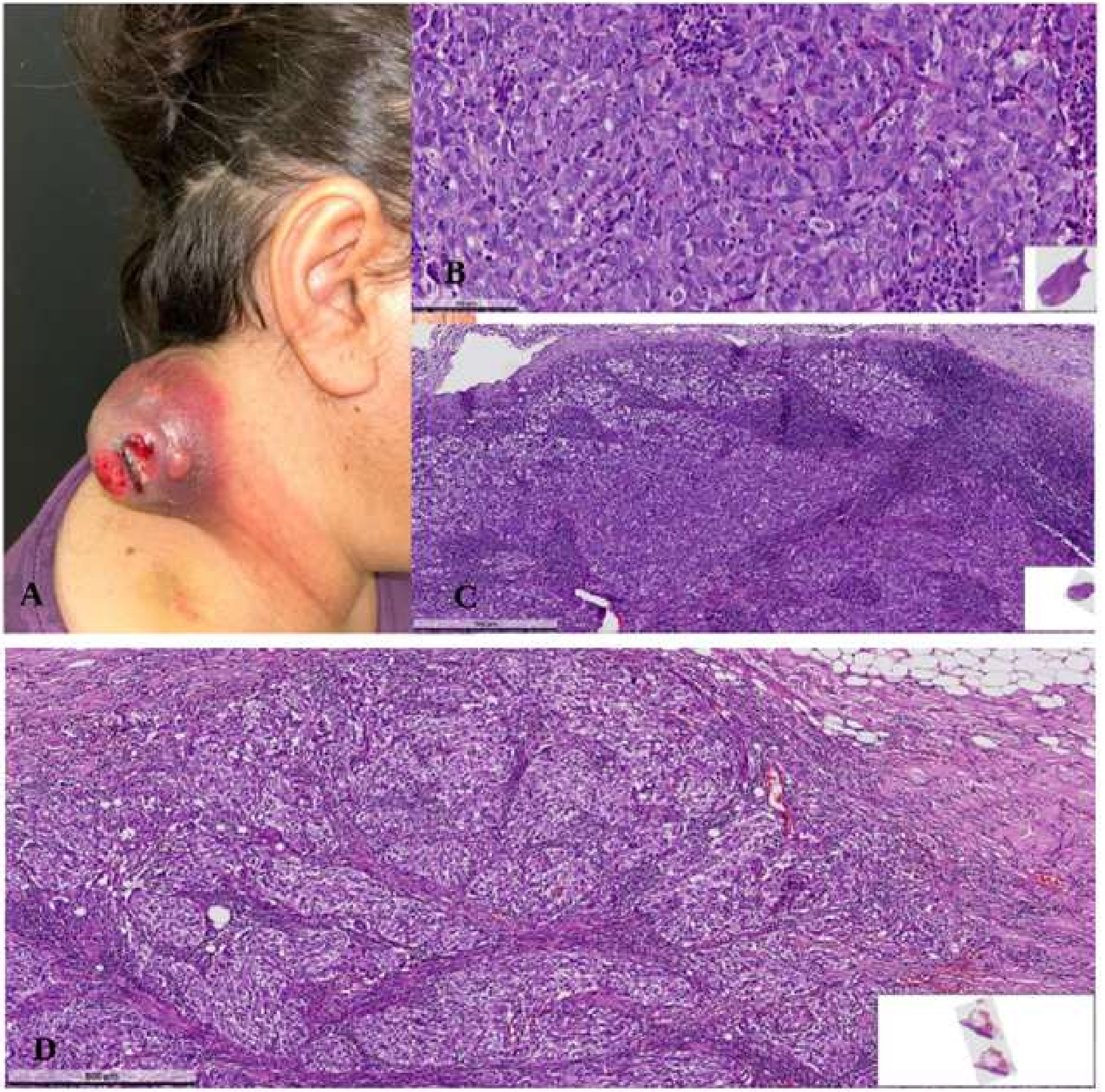






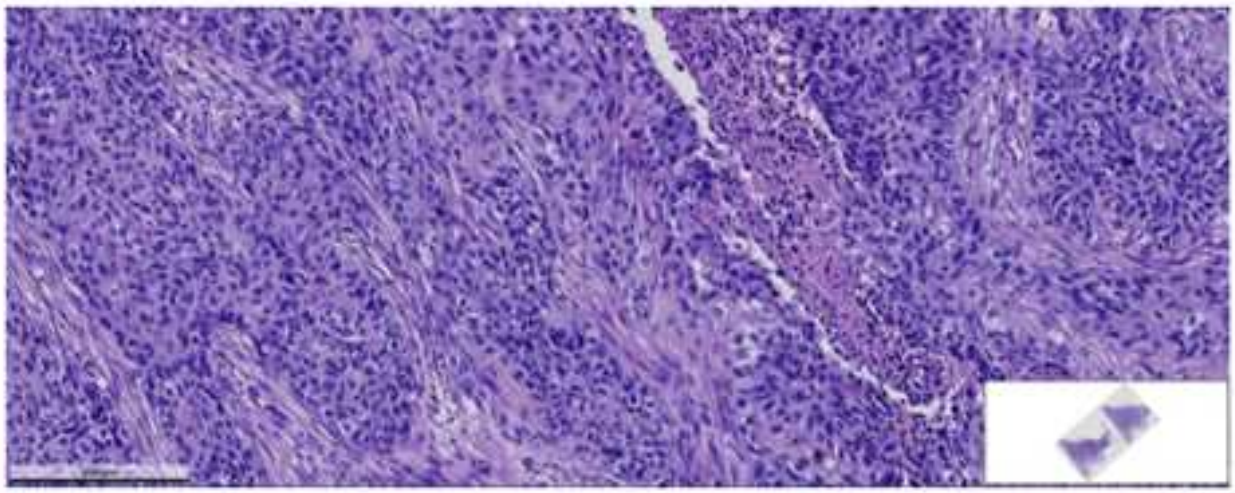
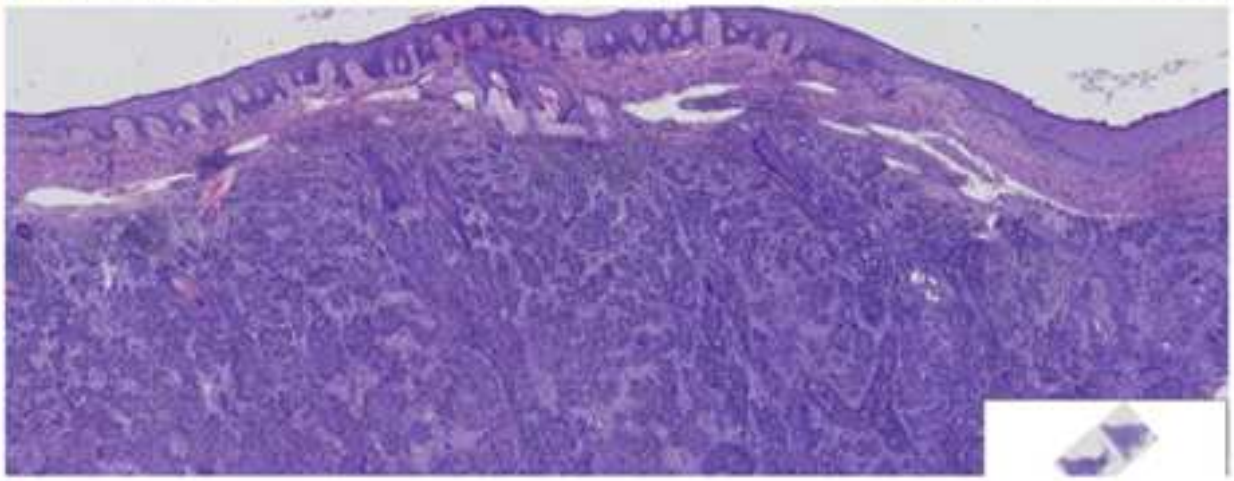
A
B
C
D


A
B
C
D
H
I
E
F
G
J


A
B
C
D



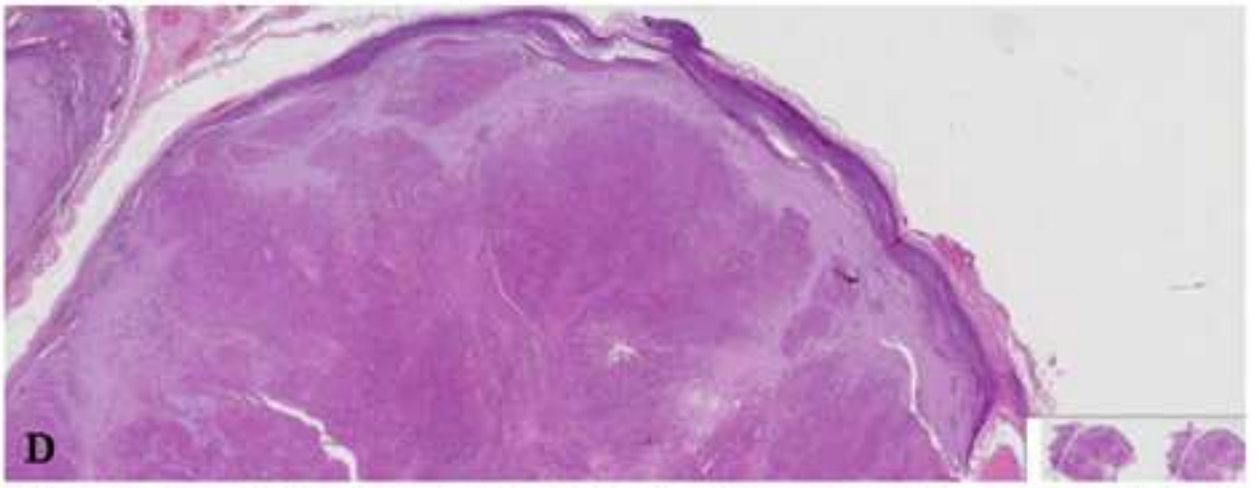


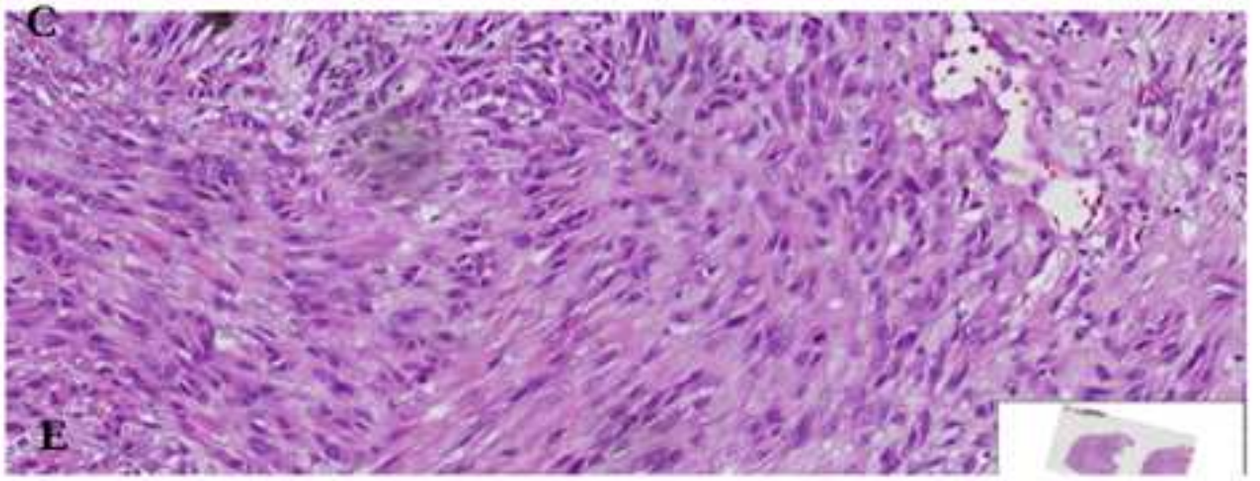




A


B


C


D


C
E

Supplementary Files

This is a list of supplementary files associated with this preprint. Click to download.

- Tablo1.docx
- Tablo2.docx
- Tablo3.docx
- Table4.docx